

Timelike geodesics of a modified gravity black hole immersed in an axially symmetric magnetic field

Saqib Hussain^{1,*} and Mubasher Jamil^{2,†}

¹*Department of Physics, School of Natural Sciences (SNS), National University of Sciences and Technology (NUST), H-12, Islamabad, Pakistan*

²*Department of Mathematics, School of Natural Sciences (SNS), National University of Sciences and Technology (NUST), H-12, Islamabad, Pakistan*

(Received 17 March 2015; published 21 August 2015)

We investigate the dynamics of a neutral and a charged particle around a black hole in modified gravity immersed in a magnetic field. Our focus is on the scalar-tensor-vector theory as modified gravity. We are interested in exploring the conditions on the energy of the particle under which it can escape to infinity after collision with another neutral particle in the vicinity of the black hole. We calculate the escape velocity of particle orbiting in the innermost stable circular orbit (ISCO) after the collision. We study the effects of modified gravity on the dynamics of particles. Further, we discuss how the presence of a magnetic field in the vicinity of a black hole affects the motion of the orbiting particle. We show that the stability of ISCO increases due to the presence of a magnetic field. It is observed that a particle can go arbitrarily close to the black hole due to the presence of a magnetic field. Furthermore, ISCO for a black hole is more stable as compared with a Schwarzschild black hole. We also discuss the Lyapunov exponent and the effective force acting on the particle in the presence of a magnetic field.

DOI: [10.1103/PhysRevD.92.043008](https://doi.org/10.1103/PhysRevD.92.043008)

PACS numbers: 97.60.Lf, 04.20.-q, 04.50.Kd, 95.30.Sf

I. INTRODUCTION

Theories of modified gravity [such as the $f(R)$ theory, Lovelock gravity, and Gauss-Bonnet theory] are constructed by adding curvature correction terms in the usual Einstein-Hilbert action through which the cosmic accelerated expansion might be explained [1] (see also [2] for reviews on modified gravity). Such correction terms give rise to solutions of the field equations without invoking the concept of dark energy. To find the dynamical equations, one can vary the action according to the metric. There is no restriction on the gravitational Lagrangian to be a linear function of Ricci scalar R [3]. Recently some authors have taken into serious consideration the Lagrangians that are “stochastic” functions with the requirement that it should be local gauge invariant [4]. This mechanism was adopted in order to treat the quantization on curved spacetime. The result was that the corrective term in the Einstein-Hilbert Lagrangian arises due to either background geometry and interactions among quantum fields or gravitational self-interaction [5]. Furthermore, it is also realized that such corrective terms should be incorporated if one wants to obtain the effective action of quantum gravity on the Planck scale [6]. Besides fundamental physical motivation, these theories have acquired a huge interest in cosmology as they exhibit inflationary behaviors and as the corresponding cosmological model seems very realistic [7,8]. In this article, our focus will be on the scalar-tensor-vector theory (will be

referred to as MOG) and the Schwarzschild-MOG black hole (MOG) [9].

Black holes can accelerate particles to arbitrarily high energy if the angular momentum of the particle is fine-tuned to some critical value (see [10] and references therein). This phenomenon is robust as it is founded on the basic properties of geodesics around a black hole [11]. Studying the dynamics of a particle (either massive or massless) around the gravitational source such as a black hole (BH) is important because it is responsible for understanding the geometrical structure of spacetime near the BH. Geodesics may display a rich structure and convey very reliable information to understand the geometry of the BH. There are many types of geodesic motion, but the circular geodesics are especially important. The exponential fade-out of a collapsing star’s luminosity can be explained by the circular geodesics as given in [12,13]. The motion of test particles helps to study the gravitational fields of objects experimentally and to compare the observations with the predictions about observable effects (light deflection, gravitational time delay, and perihelion shift).

In the surrounding of the BH, a magnetic field is generally present [14], due to the presence of plasma in the vicinity of the BH. The accretion disk or a charged gas cloud is primarily responsible for the magnetic field [15,16]. The magnetic field is stronger in the vicinity of BH’s event horizon; however, it does not affect the geometry of the BH, but the motion of the charged particle moving around a BH is affected [17,18]. The magnetic coupling process is likely responsible for the stability of the

*s.hussain2907@gmail.com

†mjamil@sns.nust.edu.pk; jamil.camp@gmail.com

black hole with its accretion disk [19]. According to this process, angular momentum and energy are transferred from the black hole to its surrounding disk. The magnetic field plays an important role in transferring sufficient energy to the surrounding particles for escaping to spatial infinity [20,21]. Other interesting processes around BHs include evaporation and phantom energy accretion onto BHs [22]. In this article, we revisit the model of Zahrani *et al.* [23] for a MOG black hole and explore the effects of modified gravity. It involves the collision of a bounded particle with an unbounded particle in the vicinity of the black hole. The main interest lies in finding the conditions of escape of a bounded particle after the collision.

The outline of the paper is as follows: In Sec. II we develop the basic equations and then derive an expression for the escape velocity of a neutral particle. In Sec. III we discuss the strength of the magnetic field, and the equations of motion of the charged particle moving around weakly magnetized MOG and the escape velocity for the particle are also calculated. The force acting on the particle is studied in Sec. IV, and geodesics of the particles moving around the MOG are discussed in Sec. V. The Lyapunov exponent is explained in Sec. VI. In Secs. VII and VIII, trajectories for the effective potential and escape velocity of the particle are presented, respectively. The conclusion is given in the last section. We will study the motion of the particle in the equatorial plane to simplify the calculations. Throughout this work we use the following metric signature $(+, -, -, -)$ and assume $c = 1$.

II. NEUTRAL PARTICLE DYNAMICS AROUND MOG BLACK HOLE

Motion of particles around a central massive object under the effect of a central force is a well-studied problem of classical mechanics (or rather Newtonian mechanics). In particular, we can think of the following problem in the present context: consider a particle of mass m moving in a circular orbit around another object of mass M such that $M \gg m$. Now for the particle to escape from the gravitational field of M , the particle's initial velocity must be more than the escape velocity. The particle can gain the escape velocity either from an external force acting on it or by hitting (or colliding) a test particle with the particle in a circular orbit. Since the collision leads to the transfer of energy as well, the particle will escape from the circular orbit if its energy after collision is more than a critical energy or escape energy. If, however, the energy of the particle after collision is smaller than the critical energy, the particle falls toward M .

The relativistic version of the above scenario was investigated by Zahrani *et al.* [23]. They studied the motion of a charged particle in the vicinity of a weakly magnetized Schwarzschild black hole and focused on the bounded trajectory lying in the black hole equatorial plane. For the charged particle to escape from the innermost circular orbit,

another particle (which is neutral and coming from a sufficiently far distance) hits the charged particle. The authors obtained the corresponding conditions of escape velocity and escape energy in the resulting process. They also predicted that the motion of the charged particle after collision will be chaotic due to the presence of the magnetic field and strong gravitational field. The chances of collision between two particles around the black hole, in general, are feeble. However, the process itself is important to describe the ejection of particles from the vicinity of black holes. Later on Hussain *et al.* [24] investigated a similar scenario for a slowly rotating Kerr black hole and discussed the conditions of escape for the particle. Jamil *et al.* [25] investigated a similar scenario for a Schwarzschild black hole surrounded by quintessence.

Recently, Moffat [9] obtained both static and nonstatic black hole solutions in the scalar-tensor-vector modified gravity, the theory which he himself proposed [26]. The theory fairly describes several astronomical and cosmological observations such as galaxy rotation curves [27] and gravitational lensing [28]. The modified gravitational field equations are given by [9,26]

$$R_{\mu\nu} - \frac{1}{2}g_{\mu\nu}R = -8\pi GT_{\mu\nu}^{\phi}, \quad (1)$$

where

$$T_{\mu\nu}^{\phi} = -\frac{1}{4\pi} \left(B_{\mu}^{\sigma} B_{\nu\sigma} - \frac{1}{4} g_{\mu\nu} B^{\sigma\beta} B_{\sigma\beta} \right),$$

and $B_{\mu\nu} = \varphi_{\nu,\mu} - \varphi_{\mu,\nu}$, where φ_{μ} is a vector field with the source charge $Q = \sqrt{\alpha G_N} M$ (see details below). The role of this vector field is to produce a large scale repulsive gravity that can cause accelerated cosmic expansion. Further, the vacuum field equations are

$$B^{\mu\nu}{}_{;\nu} = 0, \quad B_{[\mu\nu;\sigma]} = 0, \quad (2)$$

where “;” denotes the covariant derivative operation.

To solve the above system of equations, an *ansatz* for the static and spherically symmetric solution is assumed to be of the form

$$ds^2 = g(r)dt^2 - g(r)^{-1}dr^2 - r^2(d\theta^2 + \sin^2\theta d\phi^2). \quad (3)$$

The calculation yields [9]

$$\begin{aligned} g(r) &= 1 - 2\frac{GM}{r} + \alpha \frac{G_N GM^2}{r^2}, \\ G &= G_N(1 + \alpha), \quad Q = \kappa M, \\ \kappa &= \pm \sqrt{\alpha G_N}, \quad \alpha = \frac{G}{G_N} - 1, \end{aligned} \quad (4)$$

and therefore we have

$$Q = \pm \sqrt{\alpha G_N M}. \quad (5)$$

Note that α is a free parameter of the theory; hence, it yields a variable gravitational *constant*. Here M and Q are, respectively, the mass and electric charge of the black hole, and G_N is Newton's gravitational constant. In metric (3), the positive value of Q is chosen to maintain repulsive gravitational force, as it is necessary to describe the stable star. (For a stable star, the gravitational attraction should be balanced by the repulsive gravity.) This is a static, spherically symmetric, point particle solution of an electrically charged body like the Reissner-Nordstrom black hole [29,30]. For $\alpha = 0$, metric (3) reduces to the Schwarzschild metric (which is also the general relativistic limit). Like the Kerr [31] and Reissner-Nordström (RN) metrics it has two horizons:

$$r_{\pm} = G_N M (1 + \alpha \pm (1 + \alpha)^{\frac{1}{2}}). \quad (6)$$

Equation (6) corresponds to $g(r) = 0$ and will reduce to the Schwarzschild event horizon for $\alpha = 0$. The metric (3) is invariant under time translation and rotation around the symmetry axis. Thus the Killing vectors equations are [32]

$$\xi_{(t)}^{\mu} \partial_{\mu} = \partial_t, \quad \xi_{(\phi)}^{\mu} \partial_{\mu} = \partial_{\phi}, \quad (7)$$

which will give the constants of motion, where $\xi_{(t)}^{\mu} = (1, 0, 0, 0)$ and $\xi_{(\phi)}^{\mu} = (0, 0, 0, 1)$. The conserved quantities corresponding to these Killing vectors are the total energy (per unit mass) \mathcal{E} and azimuthal angular momentum L_z (per unit mass) of the moving particle at infinity. The motion of a neutral particle moving in the MOG background is described by the Lagrangian density [33],

$$\mathcal{L} = \frac{1}{2} g_{\mu\nu} \dot{x}^{\mu} \dot{x}^{\nu}. \quad (8)$$

From (4) and (8) we can say that t and ϕ are the cyclic coordinates. There exist constants of motion corresponding to these cyclic coordinates, i.e., total energy and azimuthal angular momentum. We have calculated these integrals of motion by using the Euler-Lagrange equation

$$\frac{d}{d\tau} \left(\frac{\partial \mathcal{L}}{\partial \dot{x}^{\mu}} \right) - \frac{\partial \mathcal{L}}{\partial x^{\mu}} = 0. \quad (9)$$

Therefore, using Eq. (9) for t and ϕ we have

$$\frac{dt}{d\tau} = \dot{t} = \frac{\mathcal{E}}{g(r)}, \quad (10)$$

$$\frac{d\phi}{d\tau} = \dot{\phi} = -\frac{L_z}{r^2}. \quad (11)$$

The overdot denotes the differentiation with respect to proper time τ throughout the calculations. Considering the planar motion of the particle, i.e., for $\theta = \pi/2$, the normalization condition $u^{\mu} u_{\mu} = 1$ gives

$$\begin{aligned} \dot{r}^2 &= \mathcal{E}^2 - U_{\text{eff}}, \\ U_{\text{eff}} &= \left(1 - 2 \frac{GM}{r} + \alpha \frac{G_N G M^2}{r^2} \right) \left(1 + \frac{L_z^2}{r^2} \right). \end{aligned} \quad (12)$$

The extreme values of the effective potential correspond to $\frac{dU_{\text{eff}}}{dr} = 0$. It occurs at $r = 6M$ for a Schwarzschild black hole [23]. The point where the innermost stable circular orbit (ISCO) exists is the convolution point of the effective potential [34]. In the present case, the ISCO occurs at

$$\begin{aligned} r_o &= \frac{\alpha G M^2 G_N + L^2}{3GM} - (\sqrt[3]{2}(L(L - 3GM) + \alpha G M^2 G_N)(L(3GM + L) + \alpha G M^2 G_N)) \\ &\times [3GM(-2\alpha^3 G^3 M^6 G_N^3 + 3GL^4 M^2(9G - 2\alpha G_N) - 2L^6 - 3\alpha G^2 L^2 M^4 G_N(2\alpha G_N + 9G) \\ &+ 3\sqrt{3}(G^3 L^2 M^4(-9GL^6 + 108G^3 L^4 M^2 + \alpha G_N(8L^6 - 126G^2 L^4 M^2 \\ &+ \alpha G M^2 G_N(24L^4 - 9G^2 L^2 M^2 + 8\alpha G M^2 G_N(\alpha G M^2 G_N + 3L^2))))))^{1/3}]^{-1} \\ &- \frac{1}{3\sqrt[3]{2}GM} (-2\alpha^3 G^3 M^6 G_N^3 + 3GL^4 M^2(9G - 2\alpha G_N) - 2L^6 - 3\alpha G^2 L^2 M^4 G_N(2\alpha G_N + 9G) \\ &+ 3\sqrt{3}(G^3 L^2 M^4(-9GL^6 + 108G^3 L^4 M^2 + \alpha G_N(8L^6 - 126G^2 L^4 M^2 \\ &+ \alpha G M^2 G_N(24L^4 - 9G^2 L^2 M^2 + 8\alpha G M^2 G_N(\alpha G M^2 G_N + 3L^2))))))^{1/3}). \end{aligned} \quad (13)$$

The critical energy and the azimuthal angular momentum of the particle corresponding to ISCO are

$$\mathcal{E}_o = \frac{(\alpha G M^2 G_N + r(r - 2GM))^2}{r^2(2\alpha G M^2 G_N + r(r - 3GM))}, \quad (14)$$

$$\mathcal{L}_{zo} = \frac{\sqrt{GM r^3 - \alpha G M^2 r^2 G_N}}{\sqrt{2\alpha G M^2 G_N - 3GM r + r^2}}. \quad (15)$$

We consider the case that an incoming particle collides with the orbiting particle at the ISCO, so that after collision it

will move within a new plane tilted with respect to the previous equatorial plane. However, to study the dynamics of a particle, it is convenient to use the fact that if the initial position and the tangent vector of the trajectory of the particle lies on a plane that contains the center of the body, then the entire trajectory lies on this plane. After collision, there are three possible cases depending on the collision mechanism: (i) bound motion, (ii) capture by BH, and (iii) escape to infinity. For a small change in energy and angular momentum, the orbit of the particle alters very slightly. While for large changes it may escape to infinity or capture by BH depending upon the nature of change in the path. After collision, the particle will no longer remain in the same equatorial plane, so further discussion would be dealt with respect to the new plane. But note that due to spherical symmetry all equatorial planes are equivalent. Because of the collision, the particle should have new constants of motion \mathcal{E} , L^2 , and L_z . For simplification of our problem we consider the case of collision when (i) the azimuthal angular momentum is invariant during collision and (ii) the initial radial velocity does not change. These conditions imply that only energy of the particle will change; hence, its motion would be determined by considering only the change in the energy. After collision the particle acquires an escape velocity v , in an orthogonal direction of the equatorial plane as explained in [14]. The angular momentum and energy of the particle after collision becomes (at the equatorial plan $\theta = \frac{\pi}{2}$)

$$L^2 = r_o^2 v^2 + \frac{L_{zo}^2}{\sin^2 \theta}, \quad L^2 = r_o^2 v^2 + L_{zo}^2. \quad (16)$$

Here $v \equiv -r_o \dot{\theta}_o$ and $\dot{\theta}_o$ is the initial polar angular velocity of the particle and r_o is the radius of ISCO. This velocity should be in an orthogonal direction to the equatorial plane [35]. Further,

$$\mathcal{E} = \sqrt{\left(1 - \frac{2GM}{r} + \frac{\alpha G_N G M^2}{r^2}\right) v^2 + \mathcal{E}_o^2}, \quad (17)$$

where \mathcal{E}_o is defined in Eq. (14). It is clear that these values of angular momentum (16) and energy (17) are larger than their values (14) and (15) before collision. Also Eq. (17) shows that as $r \rightarrow \infty$, $\mathcal{E} \rightarrow \mathcal{E}_o \rightarrow 1$. So for $\mathcal{E} \equiv \mathcal{E} \geq 1$ the particle will have unbound motion. In other words, the particle cannot escape to infinity if $\mathcal{E} < 1$. Hence, the necessary condition for a particle to escape to infinity after collision is $\mathcal{E} \geq 1$ or

$$v \geq \frac{\sqrt{r(2GM(L^2 + r^2) - L^2 r) - \alpha GM^2 G_N (L^2 + r^2)}}{\sqrt{r^2(\alpha GM^2 G_N + r(r - 2GM))}}. \quad (18)$$

The last expression for velocity v is obtained by solving Eq. (17) at $\mathcal{E}_{\text{new}} = 1$.

III. MOTION OF A CHARGED PARTICLE AROUND A WEAKLY MAGNETIZED SMOG BLACK HOLE

A. Magnetic field in the vicinity of BH

The magnetic coupling (MC) process is responsible for the attraction of a black hole with its accretion disk [17,19,36–38]. According to this process, angular momentum and energy are transferred from a black hole to its surrounding disk. The process of MC provides the relation between the strength of the magnetic field at the black hole horizon and its mass M and the rate of accretion \dot{M} [39]. This relation is as follows:

$$\mathcal{B}_h = \frac{1}{r_h} \sqrt{2m_p \dot{M} c}. \quad (19)$$

Here the black hole horizon r_h is given by (6) and m_p is the magnetization parameter that indicates the relative power of the process of MC with respect to disk accretion. If disk accretion is dominant over the MC process, then $m_p < 1$, and if the MC process is dominant over disk accretion, then $m_p > 1$ while $m_p = 1$ correspond to the equipartition of these two processes. The magnetic field expression is given by [39]

$$\mathcal{B}_h = (v_b f^2(\alpha, m_p))^{\frac{1}{2}} \times 10^{7.35+0.45\theta}. \quad (20)$$

The magnetic field strength at the horizon of MOG-BH is 4.93×10^8 G for $m_p = 1$, $\alpha = 0.1$, $\theta = 0.5$, and $v_b = 300$.

Similar effects of particle collision with a high center of mass energy in the vicinity of the black hole can also be possible if the black hole is nonrotating, provided there exists a magnetic field in its surrounding. There exists theoretical and experimental evidence that such a magnetic field should exist in the surrounding black hole [21–28,40]. We assume that this magnetic field is weak and its energy and angular momentum do not affect the background geometry of the black hole. The above-mentioned condition satisfies for a black hole of mass M if the magnetic field strength holds the condition [41]

$$\mathcal{B} \ll \mathcal{B}_{\text{max}} = \frac{1}{G^{\frac{3}{2}} M_{\odot}} \left(\frac{M_{\odot}}{M} \right) \sim 10^{19} \frac{M_{\odot}}{M}. \quad (21)$$

These kinds of black holes are called weakly magnetized.

B. Magnetic field calculation

In this section we explore how the presence of a magnetic field in the BH exterior stimulates the motion of a charged particle. First, we calculate the magnetic field

in the vicinity of the black hole by following the procedure as given by [23,24].

The Killing vector equation is [42]

$$\square \xi^\mu = 0, \quad (22)$$

where ξ^μ is a Killing vector. Equation (22) corresponds to the Maxwell equation for 4-potential A^μ in the Lorentz gauge $A^\mu{}_{;\mu} = 0$. Define A^μ as [43,44]

$$A^\mu = \left(\frac{\alpha GM}{r}, 0, 0, \frac{\mathcal{B}}{2} \right). \quad (23)$$

Here the magnetic field is defined as [23]

$$\mathcal{B}^\mu = -\frac{1}{2} \epsilon^{\mu\nu\lambda\sigma} F_{\lambda\sigma} u_\nu, \quad (24)$$

where

$$\epsilon^{\mu\nu\lambda\sigma} = \frac{\epsilon^{\mu\nu\lambda\sigma}}{\sqrt{-g}}, \quad \epsilon_{0123} = 1, \quad g = \det(g_{\mu\nu}). \quad (25)$$

Here $\epsilon^{\mu\nu\lambda\sigma}$ is the Levi-Civita symbol, and $F_{\mu\nu}$ is the Maxwell tensor, defined as

$$F_{\mu\nu} = A_{\nu;\mu} - A_{\mu;\nu} = A_{\nu;\mu} - A_{\mu;\nu}. \quad (26)$$

For a local observer at rest, the component of four velocity is

$$u^\mu = (u^t, 0, 0, 0) = (g(r)^{-\frac{1}{2}}, 0, 0, 0). \quad (27)$$

Here we assume $u^t > 0$, to signify the ‘‘forward-in-time’’ condition. By Eqs. (23)–(27) the magnetic field 4-vector becomes

$$\mathcal{B}^\mu = \left(0, \mathcal{B}g(r)^{\frac{1}{2}} \cos \theta, -\frac{\mathcal{B}g(r)^{\frac{1}{2}}}{r} \sin \theta, 0 \right). \quad (28)$$

The magnetic field is along with the z axis at spatial infinity, and we assume that it is directed upward [45]. At the equatorial plane only the \mathcal{B}^θ component will survive. In Fig. 1 we have plotted \mathcal{B}^θ as a function of r . It decreases initially and then becomes almost constant for large r (away from the black hole). So, it is homogeneous at $r \rightarrow \infty$.

C. Dynamical equations

The Lagrangian of the moving particle of rest mass m and electric charge q in the vicinity of MOG-BH is

$$\mathcal{L} = \frac{1}{2} g_{\mu\nu} \dot{x}^\mu \dot{x}^\nu + \frac{q}{m} A_\mu \dot{x}^\mu. \quad (29)$$

Using the Euler-Lagrange equation (27) for t and ϕ , we get

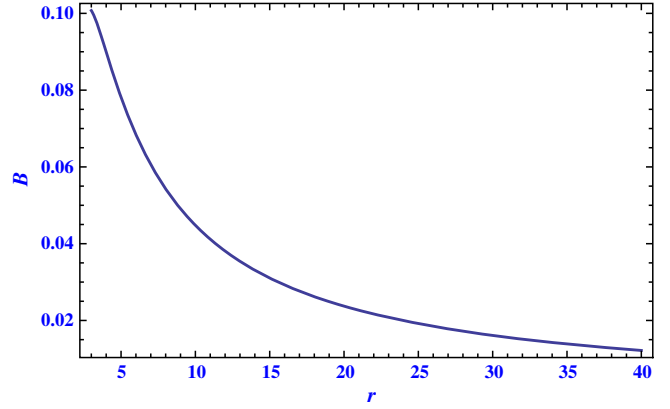


FIG. 1 (color online). The magnetic field \mathcal{B}^θ vs r for $\alpha = 0.2$.

$$g(r) \left(\dot{t} + \frac{\epsilon \alpha GM}{r} \right) = \mathcal{E}. \quad (30)$$

Here, $\epsilon = \frac{q}{m}$ is the specific charge of a particle and

$$\dot{\phi} = -\frac{L_z}{r^2 \sin^2 \theta} + B, \quad (31)$$

where

$$B \equiv \frac{\epsilon \mathcal{B}}{2}. \quad (32)$$

Using the normalization condition $u^\mu u_\mu = 1$, we obtain

$$1 = g(r) \dot{t}^2 - \frac{1}{g(r)} \dot{r}^2 - r^2 \dot{\theta}^2 - r^2 \sin^2 \theta \dot{\phi}^2. \quad (33)$$

By using Eqs. (30) and (31) in (33) and choosing $\theta = \frac{\pi}{2}$, we have

$$\dot{r}^2 + U_{\text{eff}} = \mathcal{E}^2, \quad (34)$$

and then the effective potential is

$$\mathcal{E}_\pm = U_{\text{eff}} \pm \frac{\epsilon GM}{r} \pm \sqrt{g(r) \left[1 + r^2 \left(\frac{L_z}{r^2} - B \right)^2 \right]}. \quad (35)$$

According to Eq. (16), after collision $L_z \rightarrow L$. Hence, the effective potential reduces to

$$\mathcal{E}_\pm = U_{\text{eff}} \pm \frac{\epsilon \alpha GM}{r} \pm \sqrt{g(r) \left[1 + r^2 \left(\frac{L}{r^2} - B \right)^2 \right]}. \quad (36)$$

Putting the value of L from Eq. (16) and $\mathcal{E}_\pm = 1$ in Eq. (36) and then solving for v , we get

$$v = \frac{1}{r^4(\alpha GM^2 G_N + r(r - 2GM))} [GMr^2(Br^2 - L)(\alpha MG_N - 2r) + Br^6 - Lr^4] \pm \sqrt{GMr^6(\alpha GM^2 G_N + r(r - 2GM))(\alpha^2 GM\epsilon^2 - \alpha MG_N + r(2 - 2\alpha\epsilon))}. \quad (37)$$

For a particle to escape from the black hole's vicinity, its velocity should be greater than or equal to v .

A charged particle moving in an external electromagnetic field $F_{\mu\nu}$ obeys the equation of motion:

$$\ddot{x}^\mu + \Gamma_{\nu\sigma}^\mu \dot{x}^\nu \dot{x}^\sigma = \frac{q}{m} F_{\alpha}^\mu \dot{x}^\alpha. \quad (38)$$

The dynamical equations for θ and r , respectively, are

$$\ddot{\theta} = \frac{-2}{r} \dot{r} \dot{\theta} + \frac{L_z^2 \cos \theta}{r^4 \sin^3 \theta} - B^2 \sin \theta \cos \theta, \quad (39)$$

$$\ddot{r} = \gamma - \dot{\theta}^2(\gamma r^2 - rg(r)) - \frac{L^2}{r^2 \sin^2 \theta} \left(\gamma - \frac{g(r)}{r} \right) - B^2 \sin^2 \theta (-3rg(r) + r^2 \gamma) + BL \left(2\gamma - \frac{4g(r)}{r} \right), \quad (40)$$

where $\gamma = \frac{M}{r^2} - \frac{\alpha GM^2}{r^3}$. For $\theta = \frac{\pi}{2}$ Eq. (39) is satisfied obviously and Eq. (40) becomes

$$\ddot{r} = \gamma - \frac{L^2}{r^2} \left(\gamma - \frac{g(r)}{r} \right) - B^2 (-3rg(r) + r^2 \gamma) + BL \left(2\gamma - \frac{4g(r)}{r} \right). \quad (41)$$

We have solved Eq. (41) numerically by using the built-in command of Mathematica NDSolve for $\alpha = 0.2$, $B = 0.3$, and $L_z = 2$ and plotted the solution in Fig. 2. In Fig. 2 the

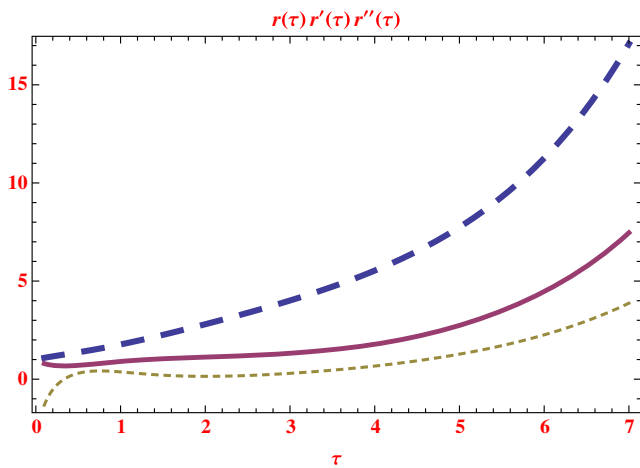


FIG. 2 (color online). Interpolating function $r(\tau)$ as the solution of Eq. (41) for $L_z = 2$, $B = 0.3$, and $\alpha = 0.2$. Here the large bold dashed curve represents $r\tau$, the solid curve is for $\dot{r}(\tau)$, and the short dashed curve corresponds to $\ddot{r}(\tau)$.

upper curve represents $r(\tau)$, the middle curve is for \dot{r} (radial velocity), and the lower one is for \ddot{r} . \dot{r} is the radial velocity that represents the escape behavior as it is increasing with the increase of r , and \ddot{r} is the radial acceleration that is analogous to the force exerted on the particle in the radial direction after the collision.

IV. FORCE ON A CHARGED PARTICLE IN THE VICINITY OF MOG-BH

As we have already calculated the effective potential for MOG-BH, we can also compute the effective force on a neutral and a charged particle by [46]

$$F = -\frac{1}{2} \frac{dU_{\text{eff}}}{dr}, \quad (42)$$

$$F = \frac{-G_N M(3L^2 + r^2) + L^2 r}{r^4} + \frac{\alpha G_N M((\alpha + 1)G_N M(2L^2 + r^2) - r(3L^2 + r^2))}{r^5}. \quad (43)$$

It can be seen from Eq. (43) that the force due to scalar tensor-vector gravity is repulsive if $(\alpha + 1)G_N M(2L^2 + r^2) > -r(3L^2 + r^2)$,

$$F = \frac{L^2 r - GM(3L^2 + r^2)}{r^4} + \frac{Q^2(2L^2 + r^2)}{r^5}. \quad (44)$$

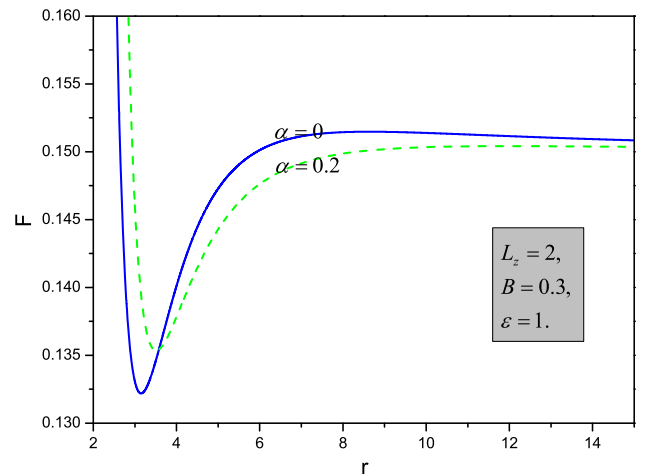


FIG. 3 (color online). Effective force as a function of r for different values of α .

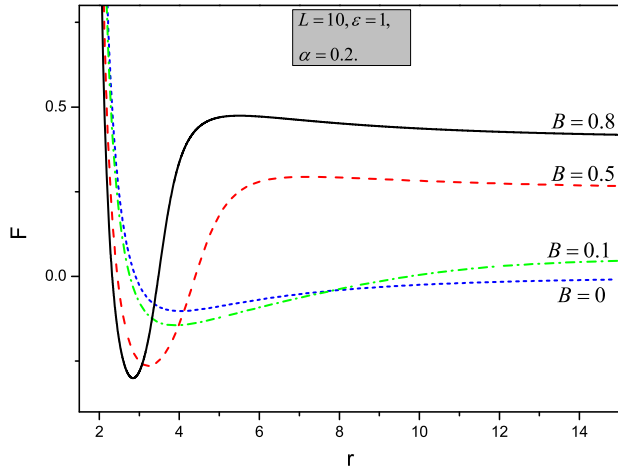


FIG. 4 (color online). Effective force against r for different values of magnetic field B .

Equation (44) represents the effective force for RN-BH, and the force due to the charge of BH is repulsive without any condition.

We are studying the dynamics of a neutral and a charged particle in the surrounding of MOG-BH where the scalar tensor-vector field produces a repulsive gravitational force that prevents a particle from falling into singularity [26]. In Fig. 3 we are comparing the effective force on a particle in the vicinity of MOG-BH with a Schwarzschild black hole. We deduce from Fig. 3 that the repulsion to reach the singularity is more for $\alpha = 0.2$ as compared to $\alpha = 0$.

To study the behavior of force against magnetic field B , we have plotted the force F as a function of r for different values of B in Fig. 4. It can be seen from Fig. 4, due to large magnetic field strength B , that force on the particle is more attractive as compared to small B .

V. COMPARISON OF GEODESICS IN THE VICINITY OF MOG-BH VS SBH

A. Geodesics of a neutral particle moving around a Schwarzschild BH

Geodesics of a particle moving toward or away from BH could be obtained by using Eqs. (10) and (12) together. We have

$$\frac{dt}{dr} = \pm \frac{\mathcal{E}}{g(r)} \frac{1}{\sqrt{\mathcal{E}^2 - U_{\text{eff}}}}. \quad (45)$$

Here U_{eff} corresponds to a neutral particle given by (12), where a positive root gives the path of the outgoing particle from the BH, and a negative root gives the path of an ingoing particle. Let us consider the particle that is coming from infinity, initially at rest, and approaches the BH. Setting $\mathcal{E} = 1$, $B = 0$, $\alpha = 0$, and $L_z = 2$ in Eq. (45), we plot the geodesics in (r, t) coordinates; see Fig. 5.

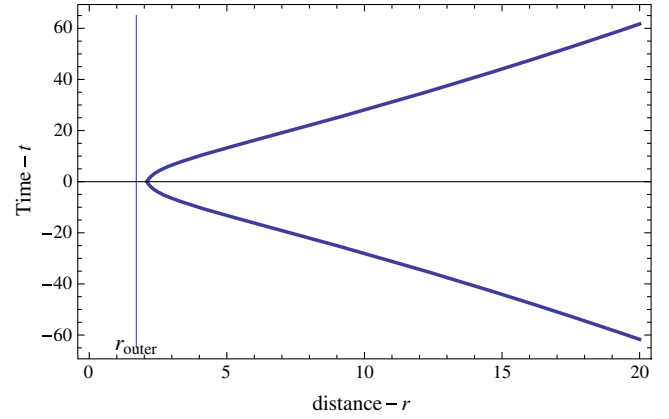


FIG. 5 (color online). Geodesic equations $\frac{dt}{dr}$ (45) against r for $\mathcal{E} = 1$, $L_z = 2$, $M = 1$.

B. Geodesics of a charged particle moving around a MOG-BH

Geodesics of the particles approaching the MOG-BH could be obtained by using Eqs. (30) and (34); together we obtain

$$\frac{dt}{dr} = \pm \sqrt{\frac{\mathcal{E}g(r)^{-1} - \frac{\epsilon\alpha GM}{r}}{\mathcal{E}^2 - U_{\text{eff}}}}. \quad (46)$$

Here U_{eff} corresponds to a charged particle given by Eq. (36) where positive and negative signs give the path of the outgoing and the ingoing particles, respectively. Setting $\mathcal{E} = 1$, $L_z = 2$, $M = 1$, in Eq. (46) we get the geodesics that are bounded by the boundaries $r = r_c$ and the outer horizon of the BH, plotted in Fig. 6. In Fig. 6, for the thick curve we consider parameter $\alpha = 0.1$, magnetic field strength $B = 0.1$, and charge of a particle $\epsilon = 0.5$, and the thin curve corresponds to $\epsilon = 1$, $B = 0.5$, and $\alpha = 0.5$. Figure 6 shows that if the strength of magnetic field B is higher, then the charged particle can reach arbitrarily close to the black hole as compared to a smaller value of B .

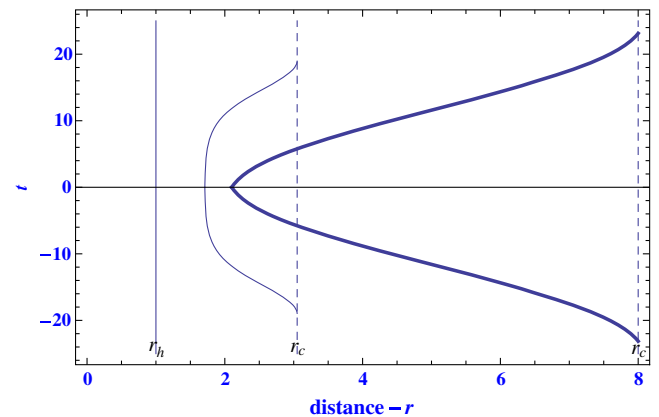


FIG. 6 (color online). Geodesic equations $\frac{dt}{dr}$ (46) against r for $\mathcal{E} = 1$, $L_z = 2$, $M = 1$.

VI. STABILITY OF ORBITS

Lyapunov exponents are the measurements of the rate of convergence or divergence of the nearby trajectories in the phase space. It is highly sensitive to the initial conditions. Its positive value is the indication of divergence among the nearby trajectories. Therefore we can check the stability of orbits by the Lyapunov exponent λ [47]. It is given by

$$\lambda = \sqrt{\frac{-U''_{\text{eff}}(r_o)}{2\dot{t}(r_o)^2}}, \quad (47)$$

where r_o is the ISCO of the particle moving around BH. In [47] a critical component for the instability is defined as

$$\gamma = \frac{T_\lambda}{T}, \quad T_\lambda = \frac{1}{\lambda}. \quad (48)$$

Here T_λ is the instability time scale. The time period for a circular orbit can be obtained from Eq. (11) in the absence of a magnetic field as

$$T = \left| \frac{2\pi r_o^2}{L_z} \right|, \quad (49)$$

and in the presence of a magnetic field, from Eq. (31) we have

$$T = \left| \frac{2\pi r_o^2}{-L_z + Br_o^2} \right|. \quad (50)$$

Here r_o is the radius of the circular orbit. We have plotted the Lyapunov exponent as a function of the magnetic field B in Fig. 7. It shows that the greater the magnetic field strength, the less λ will be. From Fig. 7 and Eq. (50) one can say that the instability of circular orbits is more for a

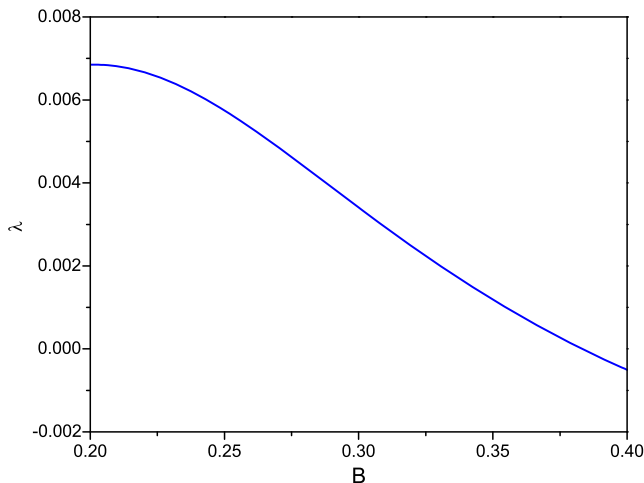


FIG. 7 (color online). The Lyapunov exponent as a function of magnetic field B for $L = 6$, $\alpha = 0.5$, $\mathcal{E} = 1$, and $\epsilon = 1$.

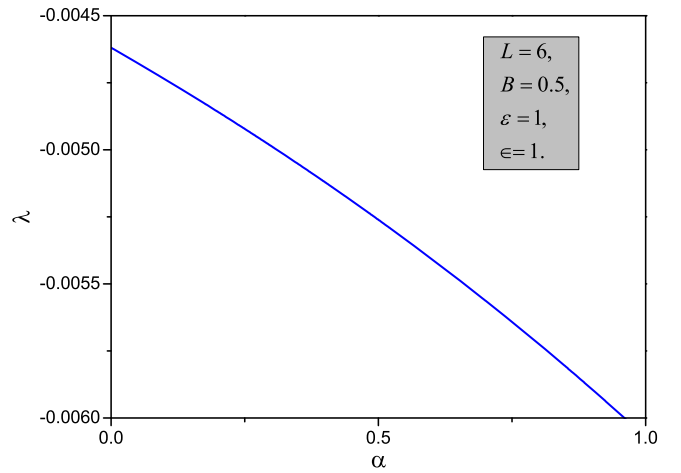


FIG. 8 (color online). The Lyapunov exponent as a function of parameter α .

Schwarzschild black hole in comparison with the black hole immersed in a magnetic field. In Fig. 8 we have also plotted λ against α , and it decreases by the increase of α . Hence, the stability of circular orbits is less for the Schwarzschild black hole as compared to the black hole with nonzero α .

VII. BEHAVIOR OF EFFECTIVE POTENTIAL

The effective potential largely depends on the g_{00} component of the metric. Therefore, before discussing the behavior of the effective potential we will compare the g_{00} component of the MOG-BH metric with the RN-BH metric as it looks similar. For the RN-BH metric,

$$g_{00} = \left(1 - \frac{2M}{r} + \frac{Q^2}{r^2} \right); \quad (51)$$

for MOG-BH from Eq. (4) we have

$$g_{00} = \left(1 - \frac{2M}{r} - 2\sqrt{\alpha}\frac{Q}{r} + \sqrt{\alpha}(1+\alpha)\frac{Q^2}{r^2} \right). \quad (52)$$

One can see that Eq. (51) contains only the Q^2 term while Eq. (52) contains Q and Q^2 . This difference leads to a large change between the behavior of the effective potentials of these two black holes. The g_{00} component of the MOG-BH metric also contains a parameter α that will create a main difference between the behavior of the potentials.

In this section we plot the effective potential and graphically explain the conditions on the energy of the particle required for an escape to infinity or for a bound motion around MOG-BH. In Figs. 9 and 10 we have plotted U_{eff} and $U_{+\text{eff}}$, respectively, corresponding to Eq. (36). Here we will discuss the long distance and short distance behavior of Eq. (36). One can see that for a small value of r the square root term will dominate, but for large r the term

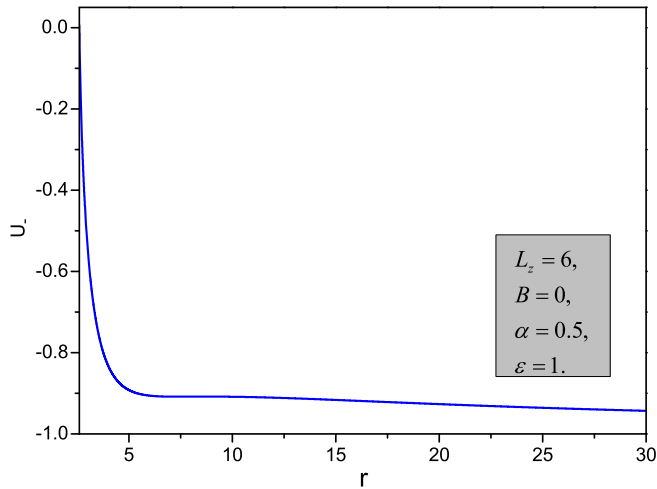


FIG. 9 (color online). Effective potential U_+ against radial coordinate r .

that is proportional to $\frac{1}{r}$ will dominate. For U_+ we get some maximum value that we have mentioned in Fig. 10 as U_{\max} . For a particle to fall into the black hole its energy should be greater than U_{\max} ; otherwise, it will bounce back to infinity or to some stable orbit. In the case of U_- , the particle can never cross the barrier as shown in Fig. 9. Hence it cannot fall into the singularity.

In Fig. 11 different regions of effective potential that correspond to the escape and the bound motion of the particle are shown. In Fig. 11, β corresponds to a region of stable orbits. If the particle has energy equal to or greater than δ , then it will fall into the black hole. U_{\max} and U_{\min} correspond to unstable and ISCO orbits, respectively. If the energy of the particle is equal to or less than β , then it will reside in one of the stable orbits. The particle having energy greater than β but less than or equal to δ can have two possibilities: either it will escape to infinity or it will be captured by the black hole. The local minima might be

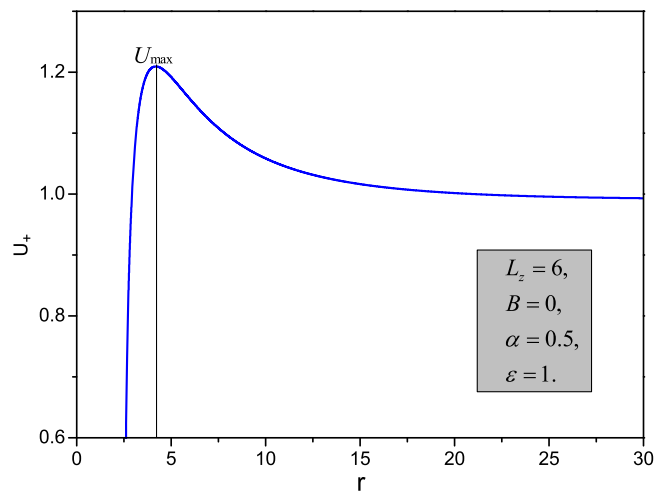


FIG. 10 (color online). Effective potential U_+ as a function of r .

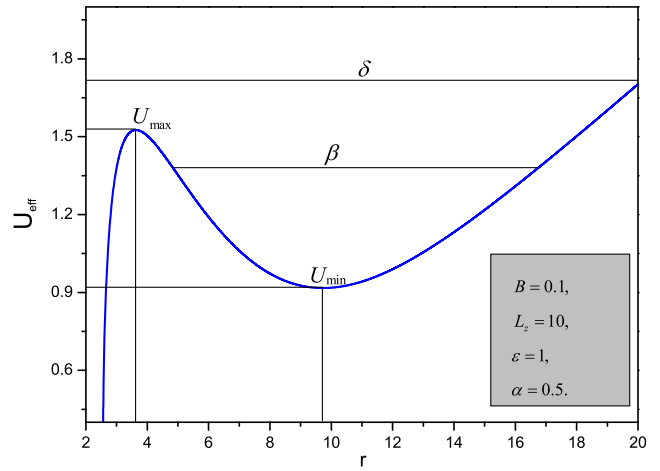


FIG. 11 (color online). Different regions of effective potential that correspond to escape and bound motion of the particle. Here β correspond to stable orbits for $b = 0.5$.

related to the change in behavior of the effective potential corresponding to BH (black brane transition) as observed in [48].

In Fig. 12 we compare the effective potential of Schwarzschild-BH, RN-BH, and MOG-BH. It can be seen from Fig. 12 that for large r all the potentials approach 1. Hence, it can be concluded that the minimum energy required for a particle to escape from the black hole vicinity is $\mathcal{E} = 1$ as we have mentioned before. Further, the maxima for the effective potential of RN-BH are greater in comparison with the maxima of effective potential of Schwarzschild-BH and MOG-BH. The particle will be captured if it has energy greater than these maxima; otherwise, it will move back to infinity or may reside in some stable orbit. Therefore, we can say that the possibility for a particle to escape from the vicinity of a black hole or to reside in some stable orbit is high in the case of MOG-BH

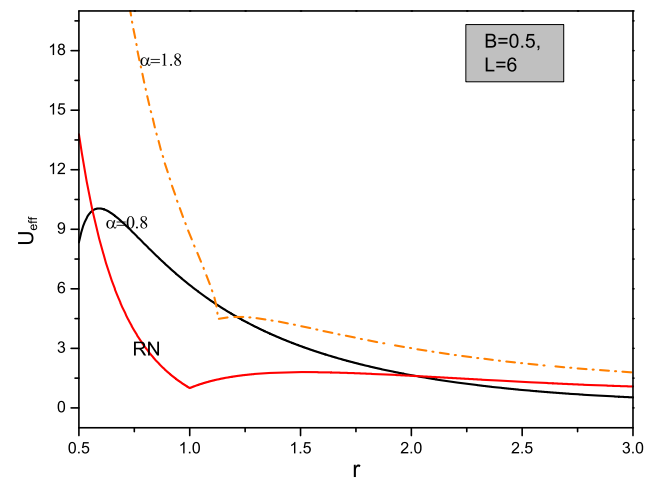


FIG. 12 (color online). Comparison of effective potential U_{eff} as a function of r . Comparison of the effective potential of RN-BH and MOG-BH.

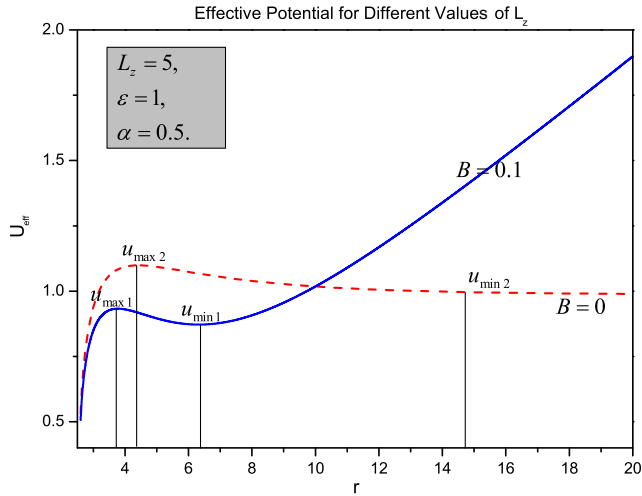


FIG. 13 (color online). Behavior of effective potentials with and without magnetic field vs r (a comparison).

with $\alpha = 1.8$ in comparison to RN-BH and MOG-BH with $\alpha = 0.8$. The particle can reach to the singularity depending upon its energy, but it cannot reach the singularity for $\alpha = 1.8$ as shown by the curve in Fig. 12. Note that $\alpha > 1$, corresponding to a naked singularity.

In Fig. 13 we compare the effective potentials in the presence with the absence of the magnetic field. In Fig. 13 $u_{\max 1}$ and $u_{\max 2}$ correspond to unstable orbits while $u_{\min 1}$ and $u_{\min 2}$ refer to ISCOs. One can notice that in the presence of the magnetic field, the minima of the effective potential are shifted toward the horizon, and the width of the stable region is also increased in comparison with the case when the magnetic field is absent. This is in agreement with [24,44]. Therefore we can say that the magnetic field acts to increase the stability of the orbits.

In Fig. 14 we have plotted the effective potential as a function of r for different values of angular momentum L_z .

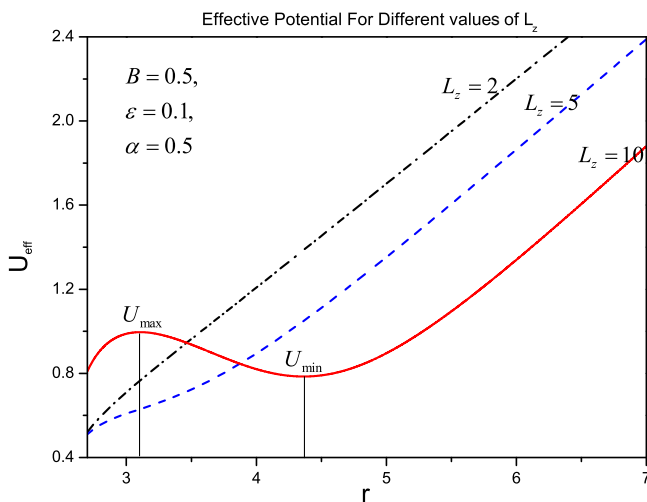


FIG. 14 (color online). Comparison of effective potentials with respect to L_z as a function of r .

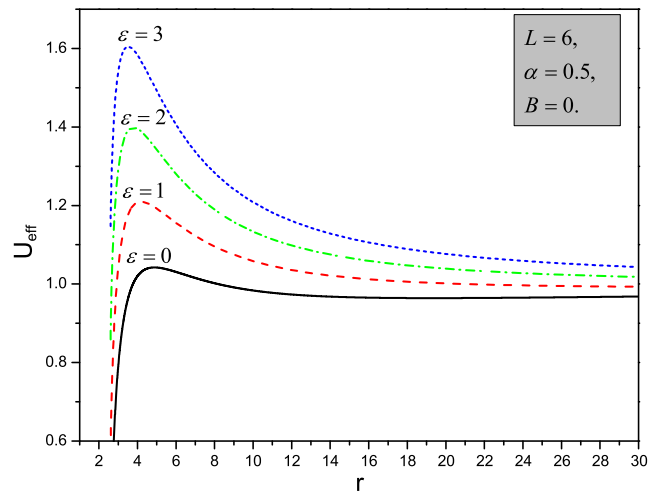


FIG. 15 (color online). Effective potential as a function of r for different values of ϵ .

One can see that for large values of L_z , the effective potential has local minima and maxima that correspond to stable and unstable circular orbits, respectively. Hence, we can say that the particle with a greater value of L_z would have a greater possibility to reside in the stable orbits in comparison with smaller values of L_z .

To study the behavior of the effective potential against ϵ , we have plotted the effective potential as a function of radial coordinate r for different values of ϵ in Fig. 15. It can be seen that the larger the value of ϵ , the greater will be the maxima of potential. Therefore, a large value of ϵ would correspond to easy escape and vice versa. It can be seen from the detailed analysis of the effective potential and the black hole physics that the scalar tensor-vector modified gravity differs from Einstein's theory of gravity a lot at a shorter distance, and it becomes similar at a long distance.

VIII. TRAJECTORIES OF ESCAPE VELOCITY

For the angular variable we have

$$\frac{d\phi}{d\tau} = -\frac{L}{r^2} + B. \quad (53)$$

If the left hand side of Eq. (53) is negative, then the Lorentz force on the particle is attractive [49]. The motion of the charged particle is in clockwise direction. The Lorentz force is repulsive if the left hand side of (53) is positive. We are not going into detail here because it is already discussed in [34,49]. Our concern is only about the action of the magnetic field on the charged particle. Therefore, the magnetic field may deform the oscillatory motion; so the greater the strength of magnetic field, the larger will be the deformation of the orbit. Hence, we can conclude that the larger the strength of the magnetic field, the easier it is for a particle to escape from the ISCO.

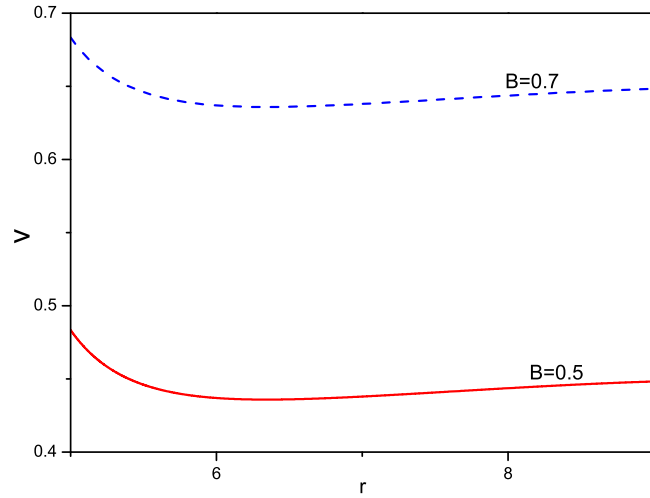


FIG. 16 (color online). Escape velocity (v) as a function of r for different values of magnetic field B .

We have also plotted in Fig. 16 the escape velocity as a function of the radial coordinate for different values of magnetic field parameter b . It can be seen that the escape velocity of the particle increases as the magnetic field strength increases, but it becomes almost constant just like the magnetic field, away from the BH. As the magnetic field is strong near the BH, therefore, we can conclude that the presence of a magnetic field will provide more energy to the particle, so that it might easily escape from the vicinity of BH. These conclusions are consistent with [15,16].

Figure 17 represents the escape velocity against radius r for different values of angular momentum L_z . From Fig. 17 we can say that the possibility for a particle to escape having a large angular momentum is small. We have plotted escape velocities for different values of α in Fig. 18, $\alpha = 0$

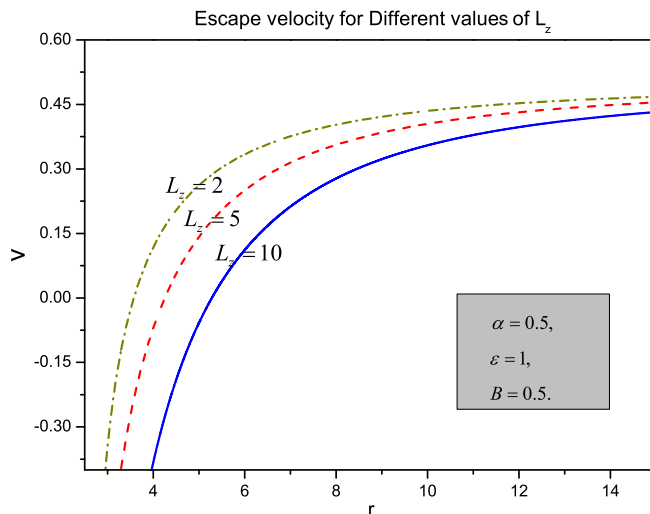


FIG. 17 (color online). Escape velocity (v) against r for different values of angular momentum ℓ .

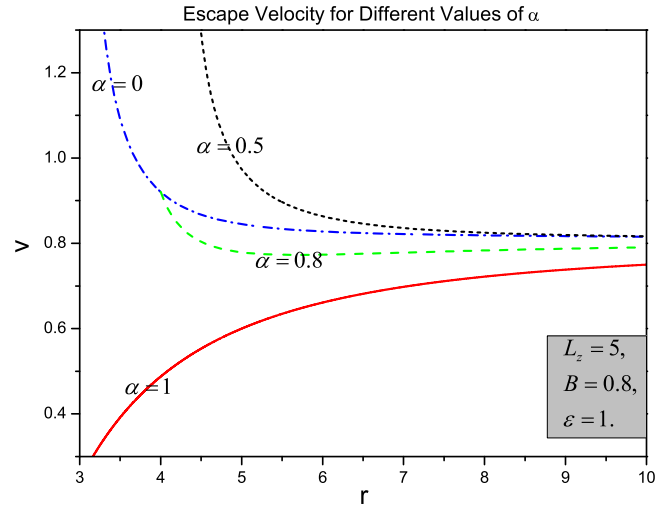


FIG. 18 (color online). Escape velocity (v) against r for different values of parameter α .

corresponding to S-BH (Schwarzschild Black Hole) and $\alpha = 1$ corresponding to RN-BH.

In Fig. 18 we compare the escape velocity of a particle moving around the S-BH, RN-BH, and MOG-BH. Note that the difference between the velocities is larger near the black hole (initially) and it becomes almost the same away from the black hole. Therefore, we can conclude that the effect of the charge of the black hole on the motion of the particle is large while it reduces as a particle moves away from it. One can see that for large r the escape velocity is the same for all values of α but for small r a lesser value of α corresponds to a greater value of the escape velocity and vice versa.

IX. SUMMARY AND CONCLUSION

We have investigated and compared the dynamics of a charged and a neutral particle in the vicinity of S-BH, RN-BH, and MOG-BH. Geodesics of a neutral and a charged particle in the vicinity of a MOG-BH are shown in Figs. 5 and 6. We see that for a charged particle there are two boundaries on the geodesics, $r = r_h$ and $r = r_c$, unlike the formal case in which a neutral particle comes from infinity and goes back to infinity before reaching the horizon, $r = r_h$, of the BH. We discussed the effective potential behavior in details regarding the stability of the orbits of the particle. We further discussed the energy condition for the particle, when it will escape or its motion remains bound. Expressions for the escape velocity of the particle moving around MOG-BH and for the magnetic field, present in the vicinity of BH due to plasma, are derived in this work. More important, a comparison is done for effective potentials, obtained in the presence and the absence of a magnetic field. It is found that the presence of a magnetic field enhances the stability of the orbits of the moving particles, due to the presence of its width of the stable

region in contrast to that we obtained in the case when the magnetic field is absent. We have also done the comparison of the effective potentials among the RN-BH, S-BH, and MOG-BH. Further we studied the stability by the Lyapunov exponent against a magnetic field and a parameter α . We conclude that the stability of orbits would increase due to the presence of the vector field considered in MOG. We deduce that the particle has to face more repulsion to reach the singularity due to the presence of a vector field as considered in MOG. But the presence of a magnetic field might increase the attractive force. It is found that a particle with a large value of angular momentum L_z would have a greater possibility to reside

in the stable orbits in comparison with a particle with a lesser value of it. Therefore, escape velocity corresponds less to a particle with a large value of L_z . Effects of magnetic field and parameter α on escape velocity are also investigated graphically. It is concluded that the presence of a magnetic field might provide sufficient energy to a particle to escape easily from the surrounding of BH.

ACKNOWLEDGMENTS

The authors would like to thank both referees and Lim Yen-Kheng for very useful comments to improve this paper.

-
- [1] C. Deffayet, *Phys. Lett. B* **502**, 199 (2001); J. S. Alcaniz, *Phys. Rev. D* **65**, 123514 (2002); S. M. Carroll, V. Duvvuri, M. Trodden, and M. Turner, *Phys. Rev. D* **70**, 043528 (2004); S. Nojiri and S. D. Odintsov, *Phys. Lett. B* **576**, 5 (2003); K. Atazadeh and H. R. Sepangi, *Int. J. Mod. Phys. D* **16**, 687 (2007); S. Nojiri, S. D. Odintsov, and M. Sami, *Phys. Rev. D* **74**, 046004 (2006); I. Navarro and K. V. Acoleyen, *J. Cosmol. Astropart. Phys.* **03** (2006) 008; S. Capozziello, *Int. J. Mod. Phys. D* **11**, 483 (2002); S. Nojiri and S. D. Odintsov, *Phys. Rev. D* **68**, 123512 (2003).
- [2] S. Capozziello and M. De Laurentis, *Phys. Rep.* **509**, 167 (2011); S. Nojiri and S. D. Odintsov, *Phys. Rep.* **505**, 59 (2011).
- [3] G. Magnano, M. Ferraris, and M. Francaviglia, *Gen. Relativ. Gravit.* **19**, 465 (1987).
- [4] J. D. Barrow and A. C. Ottewill, *J. Phys. A* **16**, 2757 (1983).
- [5] N. D. Birrell and P. C. W. Davies, *Quantum Fields in Curved Space* (Cambridge University Press, Cambridge, UK, 1982).
- [6] G. Vilkovisky, *Classical Quantum Gravity* **9**, 895 (1992).
- [7] A. A. Starobinsky, *Phys. Lett.* **91B**, 99 (1980).
- [8] D. La and P. J. Steinhardt, *Phys. Rev. Lett.* **62**, 376 (1989); D. La, P. J. Steinhardt, and E. W. Bertschinger, *Phys. Lett. B* **231**, 231 (1989).
- [9] J. W. Moffat, *Eur. Phys. J. C* **75**, 175 (2015).
- [10] A. Zakria and M. Jamil, *J. High Energy Phys.* **05** (2015) 147; I. Hussain, M. Jamil, and B. Majeed, *Int. J. Theor. Phys.* **54**, 1567 (2015).
- [11] T. Harada and M. Kimura, *Classical Quantum Gravity* **31**, 243001 (2014).
- [12] M. A. Podurets, *Astron. Zh.* **41**, 1090 (1964); [*Sov. Astron.* **8**, 868 (1965)].
- [13] W. L. Ames and K. S. Throne, *J. Astrophys. Astron.* **151**, 659 (1968).
- [14] C. V. Borm and M. Spaans, *Astron. Astrophys.* **553**, L9 (2013).
- [15] J. C. McKinney and R. Narayan, *Mon. Not. R. Astron. Soc.* **375**, 523 (2007).
- [16] P. B. Dobbie, Z. Kuncic, G. V. Bicknell, and R. Salmeron, in *Proceedings of IAU Symposium 259: Cosmic Magnetic Fields: From Planets, To Stars and Galaxies*, edited by K. G. Strassmeier, A. G. Kosovichev, and J. E. Beckman (Cambridge University Press, Cambridge, UK, 2009).
- [17] R. Znajek, *Nature (London)* **262**, 270 (1976).
- [18] V. P. Frolov and P. Krtous, *Phys. Rev. D* **83**, 024016 (2011).
- [19] R. D. Blandford and R. L. Znajek, *Mon. Not. R. Astron. Soc.* **179**, 433 (1977).
- [20] S. Koide, K. Shibata, T. Kudoh, and D. I. Meier, *Science* **295**, 1688 (2002).
- [21] S. Kide, *Phys. Rev. D* **67**, 104010 (2003).
- [22] M. Jamil and A. Qadir, *Gen. Relativ. Gravit.* **43**, 1069 (2011); B. Nayak and M. Jamil, *Phys. Lett. B* **709**, 118 (2012); M. Jamil, D. Momeni, K. Bamba, and R. Myrzakulov, *Int. J. Mod. Phys. D* **21**, 1250065(2012); M. Jamil and M. Akbar, *Gen. Relativ. Gravit.* **43**, 1061 (2011).
- [23] A. M. A. Zahrani, V. P. Frolov, and A. A. Shoom, *Phys. Rev. D* **87**, 084043 (2013).
- [24] S. Hussain, I. Hussain, and M. Jamil, *Eur. Phys. J. C* **74**, 3210 (2014).
- [25] M. Jamil, S. Hussain, and B. Majeed, *Eur. Phys. J. C* **75**, 24 (2015).
- [26] J. W. Moffat, *J. Cosmol. Astropart. Phys.* **03** (2006) 3004.
- [27] J. W. Moffat, arXiv:1101.1935; J. W. Moffat and V. T. Toth, *Galaxies* **1**, 65 (2013); arXiv:1005.2685; *AIP Conf. Proc.* **1241**, 1066 (2010).
- [28] J. W. Moffat and V. T. Toth, *Mon. Not. R. Astron. Soc.* **397**, 1885 (2009).
- [29] G. Nordstorm, *Proc. Kon. Ned. Akad. Wet.* **29**, 1238 (1918).
- [30] H. Reissner, *Ann. Phys. (Berlin)* **355**, 106 (1916).
- [31] R. P. Kerr, *Phys. Rev. Lett.* **11**, 237 (1963).
- [32] T. Igata, T. Koike, and H. Ishihara, *Phys. Rev. D* **83**, 065027 (2011).
- [33] L. D. Landau and E. M. Lifshitz, *The Classical Theory of Fields* (Pergamon Press, Oxford, 1975).
- [34] S. Chandrasekher, *The Mathematical Theory of Black Holes* (Oxford University Press, New York, 1983).

- [35] B. Punsly, *Black Hole Gravitohydrodynamics* (Springer-Verlag, Berlin, 2001).
- [36] D. X. Wang, K. Xiao, and W.-H. Lei, *Mon. Not. R. Astron. Soc.* **335**, 655 (2002).
- [37] D.-X. Wang, R.-Y. Ma, W.-H. Lei, and G.-Z. Yao, *Astrophys. J.* **595**, 109 (2003).
- [38] W. M. Zhang, Y. Lu, and S. N. Zhang, *Chin. J. Astron. Astrophys.* **5**, 347 (2005).
- [39] M. Yu. Piotrovich, N. A. Silant, Yu. N. Gnedin, and T. M. Natsvlishvili, [arXiv:1002.4948v1](https://arxiv.org/abs/1002.4948v1).
- [40] V. Frolov, *The Galactic Black Hole*, edited by H. Falcke and F. H. Hehl (IOP, London, 2003).
- [41] V. P. Frolov, *Phys. Rev. D* **85**, 024020 (2012).
- [42] R. M. Wald, *Phys. Rev. D* **10**, 1680 (1974).
- [43] A. A. Abdujabbarov, B. J. Ahmedov, and N. B. Jurayeva, *Phys. Rev. D* **87**, 064042 (2013).
- [44] A. N. Aliev and N. Ozdemir, *Mon. Not. R. Astron. Soc.* **336**, 241 (2002).
- [45] H. Q. Hong, C. J. Hua, and W. Y. Jiu, *Chin. Phys. Lett.* **31**, 060402 (2014).
- [46] S. Fernando, *Gen. Relativ. Gravit.* **44**, 1857 (2012).
- [47] V. Cardoso, A. S. Miranda, E. Berti, H. Witek, and V. T. Zanchin, *Phys. Rev. D* **79**, 064016 (2009).
- [48] R. Emparan and R. C. Myers, *J. High Energy Phys.* **09** (2003) 025.
- [49] V. P. Frolov and A. A. Shoom, *Phys. Rev. D* **82**, 084034 (2010).